Surface Dynamics of Liquids in Nanopores

J.-P. Korb,[1] L. Malier,[1,*] F. Cros,[1] Shu Xu,[2] and J. Jonas[2]
[1]*Laboratoire de Physique de la Matière Condensée, C.N.R.S., Ecole Polytechnique, 91128 Palaiseau, France*
[2]*Department of Chemistry, University of Illinois, Urbana, Illinois 61801*
(Received 22 April 1996)

^{2}H NMR relaxation of a selectively deuterated polar molecule confined to a set of calibrated nanoporous silica glasses is reported. These experiments, combined with the consideration of different time scales in the theory of surface relaxation, show how confinement effects can provide detailed information on the rotational dynamics of temporarily adsorbed liquid layers in presence of biphasic fast exchange. In particular, the results show the existence of an orientational order parameter within the wetting monolayer. [S0031-9007(96)01130-1]

PACS numbers: 81.05.Rm, 68.45.–v, 76.60.Es

What are the structure and dynamics of a liquid layer near a solid boundary surface? This question is of fundamental importance for the study of liquids in porous media, liquid crystals, and membranes. This is all the more important as a liquid confined to a region that approaches molecular dimensions has dynamic and thermodynamic properties strongly changed relatively to the bulk. Examples include anomalous [1] and lamellar diffusions [2], enhancement of correlation times [3], shifts of melting and freezing temperatures [4,5], orientational ordering, and molecular dynamics of liquid crystals confined in submicron cavities [6,7]. This question is also of technological significance for heterogeneous catalysis, membrane separation, lubrication, and oil recovery. So far, the dynamics of such a wetting layer has not been fully determined because of its small fraction and its chemical exchange with the rest of the liquid. A surface partial ordering and slower dynamics have been evidenced in confined liquid crystals where ^{2}H quadrupolar splitting persists, even in the isotropic phase [7]. However, for simple liquids, such spectroscopic features cannot be observed due to complete motional averaging, and therefore a different approach must be developed.

In this Letter, we propose a new method to obtain information on the structure and rotational dynamics of simple polar liquids at the surface of nanopores. Our method is based on a clear separation of surface $(1/T_{1s})$ and bulk $(1/T_{1b})$ contributions of the overall ^{2}H nuclear relaxation rate $(1/T_1)$ of a polar liquid confined to a set of calibrated nanoporous silica glasses. The temperature dependences of $(1/T_{1s})$ and the selective deuterium labeling have allowed us to isolate and quantify, for the first time, anisotropic activated and nonactivated molecular motions at the pore surface. This is a new result different from the isotropic and activated molecular motions observed in bulk. An original model of anisotropic rotational dynamics of polar molecules linked by hydrogen bonds on the pore surface has been proposed. It is based on fast and slow (activated and nonactivated) rotational motions. These different time scales in the theory of surface relaxation allows us to estimate the orientational order parameter as well as the complete rotational dynamics at the liquid-solid interface even in the presence of a biphasic fast exchange with the bulk liquid.

When the liquid interacts strongly with the surface, as for a polar liquid in contact with a solid surface, there are two distinct phases: a surface-affected liquid phase of thickness ε and a bulk liquid phase. Our earlier NMR studies [8] proved the applicability of the biphasic fast exchange model [9] for the analysis of the observed exponential relaxation $(1/T_1)$ for polar liquid in cylindrical pores of radius R

$$\frac{1}{T_1} = \frac{1}{T_1^b} + \frac{2\varepsilon}{R}\left(\frac{1}{T_1^s} - \frac{1}{T_1^b}\right). \tag{1}$$

The calibrated porous samples are silica glasses, prepared as previously described [8]. EPR measurements have revealed no paramagnetic impurities which would have made the relaxation analysis quite difficult. The surface of these porous glasses exhibits approximately two to three Si-O-H groups per nm^2. The samples were filled with pyridine using a bulb-to-bulb method [8]. The experiment and surface dynamics analysis we describe here are general and not limited to pyridine, but this liquid offers several advantages which make it a good model case. First, being strongly polar, it ensures to be in the wetting limit; second, its molecular rigidity prevents internal motions to contribute to the nuclear relaxation; last, it allows selective labeling. For the spin probe, we chose deuterium (^{2}H) because its relaxation proceeds through molecular reorientations. In the extreme narrowing limit, the relaxation rate $1/T_1$ is simply proportional to the reorientational correlation time [10]. Selectively deuterated pyridines were prepared from corresponding bromopyridines following literature procedures [11]. Deuterium relaxation times T_1 was measured by the inversion-recovery technique at a Larmor frequency of 27.6 MHz on a home-built spectrometer. In Eq. (1), ε corresponds to the hard sphere diameter of the pyridine molecule (0.5 nm [12]). The dynamical properties have been studied for temperature varying from -9 to 37 °C.

 0031-9007/96/77(11)/2312(4)$10.00

The benefit of selective labeling clearly appears in Fig. 1, which presents the pore radius dependences of the ^{2}H relaxation rates at different temperatures, for both *ortho* or *para* deuterium substitution. The net difference between these two rates is the experimental evidence of the anisotropy of the molecular reorientations. The linear dependence of $1/T_1$ with $1/R$ is clearly verified. This validates Eq. (1) to calculate the surface relaxation rates $1/T_1^s$.

The temperature dependences of $1/T_1^s$ for both deuterium substitutions are displayed at the top of Fig. 2. For the sake of comparison, the bulk relaxation rates $1/T_1^b$ have also been plotted. Inspection of Fig. 2 leads to the following conclusions. First, the surface relaxation rates are more than one decade larger than the bulk rates, providing evidence of a much slower dynamics at surface. Second, the ratio between *ortho* and *para* substituted pyridine relaxation times is very different between both cases. It reveals a near isotropy in the bulk dynamics as well as large temperature dependent anisotropy at surface. Moreover, the apparent activation energy associated with $1/T_1^s(para)$, estimated at 2.1 kJ mol^{-1}, is of the order of the thermal energy, thus ruling out any activated reorientational process. This is specifically important as it shows unambiguously that the chemical exchange between the surface layer and the bulk is not responsible for the surface relaxation. T_1^s is then only sensitive to the dynamics within the wetting layer. This temperature dependence cannot be explained by the usual theory of nuclear relaxation, which links $1/T_1$ and the diffusion coefficients and does not take into account any restriction in the motion [13].

We now propose a theoretical model which considers the effects of the proximity of the pore solid surface on the local anisotropic reorientational molecular motions. This will allow one to account quantitatively for the experimental results shown in Fig. 2.

The liquid-surface interactions of the pyridine molecules proceed through hydrogen bonding between the SiOH groups on the surface and the nitrogen atom. This allows for the definition of the molecular symmetry axis ($\mathbf{C}_2$), going from the nitrogen atom to the *para* carbon. Relative to the OH axis, the molecular rotational dynamics is described by a dynamical tensor whose three principal values of diffusion coefficients are $D_{\|}^s$, corresponding to rotations around the $\mathbf{C}_2$ axis of the molecule, and $D_{\perp 1}^s$ and $D_{\perp 2}^s$, related to swinging motions of this $\mathbf{C}_2$ axis, respectively, in and out of the molecular plane. The OH dipole is an instantaneous director $\mathbf{n}(t)$, making an angle $\zeta \sim 70°$ relative to the local normal director $\mathbf{n}_0$ defined by the Si-O bond of the silicon oxide surface. This director $\mathbf{n}(t)$ can freely rotate around $\mathbf{n}_0$, but due to the large momentum of inertia this motion is slow as compared to the rotation of $\mathbf{C}_2$ around $\mathbf{n}(t)$ and will further be referred as the "slow motion." The hydrogen bond is characterized by an electrostatic dipole-dipole interaction U, which depends only on the angle $\beta(t)$ between $\mathbf{n}(t)$ and the molecular dipole lying along $\mathbf{C}_2$.

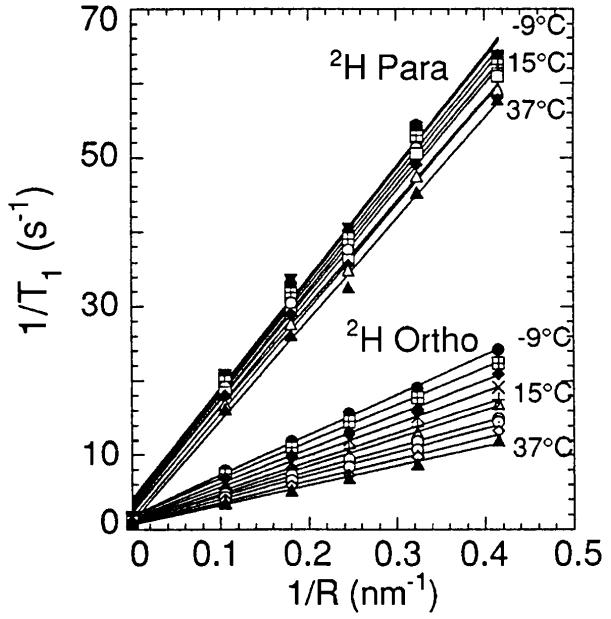

FIG. 1. The ^{2}H spin-lattice relaxation rates $1/T_1$ of liquid pyridine selectively deuterated in *ortho* and *para* as function of pore radius ($1/R$) in porous sol-gel silica glasses with $R \in \{\infty$(bulk), 9.5, 5.6, 4.1, 3.1, and 2.4 nm$\}$ at temperatures -9, -5, 0, 5, 10, 15, 20, 25, 30, and 37 °C downwards. The different lines correspond to the best fits obtained according to Eq. (1) with $\varepsilon = 0.5$ nm.

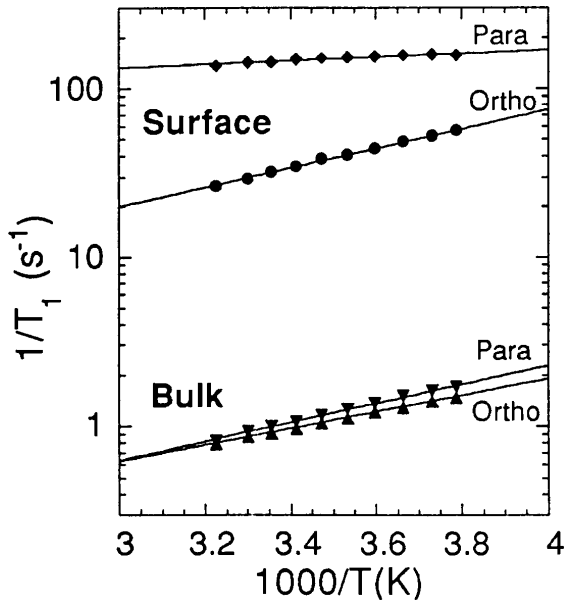

FIG. 2. Semilogarithmic plot of the surface ^{2}H spin-lattice relaxation rates $1/T_1^s(ortho)$ and $1/T_1^s(para)$ of liquid pyridine d_1 as function of inverse of temperature in porous sol-gel silica glasses (top). The corresponding bulk rates are also given (bottom). The experimental points are obtained from the slopes and intercepts of Fig. 1 according to Eq. (1). The continuous lines are the best fits obtained with Eqs. (3) and (4).

Then $U = -E_H \cos\beta$, where E_H is the bonding energy in alignment of the two dipoles. The angular distribution of the ensemble of surface molecules is described by a Boltzmann distribution $P_{eq}(\beta) \propto \exp[E_H \cos\beta/\mathcal{R}T]$ at a given temperature T.

As known, the deuterium nuclear spin relaxes through the fluctuations of the quadrupolar Hamiltonian $H_Q(t)$ due to molecular reorientation [10]. As the dynamics within the adsorbed layer is restricted, $H_Q(t)$ tends to a nonzero time-averaged value $\langle H_Q(t)\rangle$ at long times [14]. For instance, the fast (f) rotational diffusion of the $\mathbf{C}_2$ axis around $\mathbf{n}$ leads to $\langle H_Q(t)\rangle_f$ on time scales of the order of $1/D^s_\parallel$, $1/D^s_{\perp 1}$, or $1/D^s_{\perp 2}$. Similarly, the slow motion of $\mathbf{n}(t)$ around $\mathbf{n}_0$ leads to $\langle H_Q\rangle_s \equiv \langle\langle H_Q(t)\rangle_f\rangle_s$ on time scale longer than the various $1/D^s$. In the calculation of $1/T^s_1$, the squared modulus of the fluctuating part of $H_Q(t)$ must then be reduced from $\langle|H_Q(t)|^2\rangle$ to either $\langle|H_Q(t)|^2\rangle_f - |\langle H_Q(t)\rangle_f|^2$ or $\langle|\langle H_Q(t)\rangle_f|^2\rangle_s - |\langle H_Q\rangle_s|^2$ for fast and slow motions, respectively. Because of the axial symmetry about the $\mathbf{n}$ and $\mathbf{C}_2$ axes, only a single Euler angle $\beta(t)$ is needed in the calculation of $\langle H_Q(t)\rangle_f$. Of course, we average orientationally over the angle between $\mathbf{n}_0$ and the constant magnetic field $\mathbf{B}_0$. Assuming no correlation between fast and slow fluctuations, $1/T^s_1$ is the superposition of the fast and slow relaxation rates: $\langle 1/T^s_1\rangle_f + \langle 1/T^s_1\rangle_s$. Calculations similar to those encountered in liquid crystals [14] and macromolecules [15] lead to the following expressions for $\langle 1/T^s_1\rangle_f$ and $\langle 1/T^s_1\rangle_s$, valid for both *ortho* and *para* substitutions:

$$\left\langle \frac{1}{T^s_1} \right\rangle_f = \frac{3}{8}\left[\frac{e^2qQ}{\hbar}\right]^2\left[\frac{[(3\cos^2\theta - 1)^2/4][1 - \langle[3\cos^2\beta(t) - 1]/2\rangle^2_f]}{6D^s_\perp} + \frac{3\sin^2\theta\cos^2\theta}{5D^s_\perp + D^s_\parallel} + \frac{\frac{3}{4}\sin^4\theta}{2D^s_\perp + 4D^s_\parallel}\right], \quad (2a)$$

$$\left\langle \frac{1}{T^s_1} \right\rangle_s = \frac{3}{8}\left[\frac{e^2qQ}{\hbar}\right]^2 \frac{[(3\cos^2\theta - 1)^2/4]\langle[3\cos^2\beta(t) - 1]/2\rangle^2_f[1 - \langle(3\cos^2\zeta - 1)/2\rangle^2_s]}{6D^s_{\text{slow}}}. \quad (2b)$$

Here $e^2qQ/\hbar$ is 2π times the nuclear quadrupole coupling constant, which is 178 kHz for ^{2}H in pyridine (assuming the same value for *ortho* and *para* positions). θ is the angle between $\mathbf{C}_2$ and the *efg* symmetry axis (along the C-^{2}H bond). D^s_{slow} represents the isotropic diffusion coefficient for the slow motion of the SiOH around $\mathbf{n}_0$. In Eq. (2a) we have assumed that $D^s_{\perp 1}$ and $D^2_{\perp 2}$ were much smaller than $D^s_\parallel$, thus producing axial degeneracy in the dynamical tensor and leaving $D^s_\parallel$ and $D^s_\perp$ for principal values. This hypothesis will be justified later, when we show that only this assumption can account for the experimental values of T^s_1 and their respective ratio $T^s_1(ortho)/T^s_1(para)$.

In Eqs. (2), $\langle[3\cos^2\beta(t) - 1]/2\rangle_f$ is the residual time-averaged orientational term calculated over the fast motion. It represents an order parameter S_f with values between $-\frac{1}{2}$ and 1 and only depends on $x = E_H/\mathcal{R}T$. It can be calculated over $P_{eq}(\beta)$ with $0 \le \beta \le \pi/2$, as

$$S_f(x) = [e^x(2x^2 - 6x + 6) + x^2 - 6]/2x^2(e^x - 1). \quad (3)$$

This order parameter S_f is higher as the ordering energy E_H gets higher. Similarly, Eq. (2b) exhibits an order parameter for the slow motion: $S_s = \langle(3\cos^2\zeta - 1)/2\rangle_s$. Its value is imposed by the angle of the (Si-O-H) bond ($\zeta \sim 70°$) and gives a negligible contribution $S^2_s \sim 0.1$ to Eq. (2b).

Equations (2) and (4) give the relaxation rates in *ortho* and *para* substituted ($\theta = 0$ and $\theta = 2\pi/3$). These equations clearly show the importance of selective deuteration for characterization of the complex motions of the adsorbed molecules. On one hand, the surface relaxation rate of pyridine-*d*-*para* is sensitive to the rotation of $\mathbf{C}_2$ around $\mathbf{n}(t)$ as well as to the slow wobbling around $\mathbf{n}_0$ (through $D^s_\perp$ and D^s_{slow}). On the other hand, a linear combination of pyridine *ortho* and *para* deuterium relaxation rates is only dependent on the fast axial and swinging rotations ($D^s_\parallel$ and $D^s_\perp$):

$$\frac{1}{T^s_1(para)} = \frac{3}{8}\left[\frac{e^2qQ}{\hbar}\right]^2\left(\frac{1 - S^2_f}{6D^s_\perp} + \frac{S^2_f}{6D^s_{\text{slow}}}\right), \quad (4a)$$

$$\frac{1}{T^s_1(ortho)} = \frac{1}{64T^s_1(para)} + \frac{27}{128}\left[\frac{e^2qQ}{\hbar}\right]^2 \times \left[\frac{1}{5D^s_\perp + D^s_\parallel} + \frac{3/4}{2D^s_\perp + 4D^s_\parallel}\right]. \quad (4b)$$

At that point, one has to remember that $D^s_\perp$ quantifies the restricted diffusion inside a potential well defined by the hydrogen bond energy and D^s_{slow} is related to free diffusion. The numerical simulations we have performed show that the characteristic time (1/D) of such diffusions varies very little with the temperature and can be considered as constant over the explored temperature range. Hence the thermal variation of $T^s_1(para)$ is driven by the orientational order parameter S_f, which decreases when the temperature raises, according to Eq. (3).

The experimental increase of $T^s_1(para)$ with temperature then proves that the overall molecular motion around $\mathbf{n}_0$ determines this relaxation rate, thus confirming the assumption that D^s_{slow} is lower than $D^s_\perp$. Similarly, the experimental Arrhenius behavior of the combination $[1/T^s_1(ortho)\text{-}1/64T^s_1(para)]$ indicates that the activated rotation around the molecular symmetry axis $\mathbf{C}_2$ drives the left term of Eq. (4b). This shows that $D^s_\parallel$ is much larger than $D^s_\perp$.

In view of these observations, the experimental $T^s_1(para)$ gives the diffusion coefficient D^s_{slow} as well as

the hydroxyl-pyridine hydrogen bond energy E_H which determines the amplitude of S_f. Similarly, $T_1^s(ortho)$ gives the value of $D_\parallel^s$ together with the activation energy $E_\parallel^s$ of the rotation around $\mathbf{C}_2$. Fig. 2 shows the quality of the fits which give a hydrogen bond energy E_H of 15.06 kJ mol^{-1} and $D_{\text{slow}}^s = 2\,10^8$ rad^2 s^{-1}. Let us point out that this value of E_H is in agreement with the value for usual hydrogen bonds. As it is E_H which restricts the wobbling of $\mathbf{C}_2$ around $\mathbf{n}(t)$, it determines the order parameter S_f, which ranges from 0.55 to 0.64 [Eq. (3)]. This S_f implies that $\mathbf{C}_2$ wobbles in a cone whose semi-apperture varies from $2\pi/9$ at low temperature to $\pi/4$ at 37 °C.

The rotation around $\mathbf{C}_2$ is characterized by an activation energy $E_\parallel^s$ of 14.64 kJ mol^{-1} and $D_\parallel^s$ ranges from 4.10^9 to 16.10^9 rad^2 s^{-1}. Last, $D_\perp^s$ can only be defined within an interval [5.10^8, 9.10^8 rad^2 s^{-1}]. It is interesting to compare these values with the bulk values which can be obtained from Eqs. (4) with $S_f = 0$ (unrestricted motions) and with activated diffusion for $D_\parallel^b$ and $D_\perp^b$. This gives $D_\parallel^b$ ranging from 5×10^{10} to 12.5×10^{10} rad^2 s^{-1} and $D_\perp^b$ from 4×10^{10} to 12×10^{10} rad^2 s^{-1}, with their respective activation energies being 7.1 and 10.9 kJ mol^{-1}. The values found for the surface dynamics illustrate the slowing down of the dynamics caused by solid-liquid interactions and how the activation energies increase with the steric hindrance due to adsorbed neighbor molecules. This trend agrees with our observations for other polar molecules in confinement. The seemingly paradoxical behavior of activation energy found in previous study on totally deuterated polar molecules [8] was then only due to an overall mixing of all the deuterium relaxation times.

In conclusion, this experiment shows how confinement effects can provide detailed information on the dynamics of temporarily adsorbed layers. Even when the two populations (adsorbed and bulk) are in fast exchange and prevent spectroscopic resolution, confinement allows one to study the surface layer dynamical parameters. Thanks to selective labeling, NMR relaxation allows one to determine the anisotropy of the motions at surface.

In the case of pyridine on a wetting surface, we have shown how rotation around the molecular axis is hindered by neighboring molecules and that this molecular axis explores a narrow cone which opens slightly as the temperature increases. This molecular ensemble is also in slow rotational motion around the local normal to the surface. The various diffusion coefficients have been determined. The proposed method could be easily generalized to other polar molecules.

This work was supported in part by the Air Force Office of Scientific Research under Grant No. F49620-93-1-0241 and by the National Science Foundation under Grant No. NSF CHE 95-26237.

*To whom correspondence should be addressed.

[1] R. Kimmich *et al.,* Appl. Magn. Reson. **4**, 425 (1993).
[2] J.-P. Korb, Shu Xu, and J. Jonas, J. Chem. Phys. **98**, 2411 (1993); J.-P. Korb *et al., ibid.* **101**, 7074 (1994).
[3] S. Stapf, R. Kimmich, and R. O. Seitter, Phys. Rev. Lett. **75**, 2855 (1995).
[4] R. Mu and V. M. Malhotra, Phys. Rev. B **46**, 532 (1992).
[5] J. H. Strange, M. Rahman, and E. G. Smith, Phys. Rev. Lett. **71**, 3589 (1993).
[6] S. Žumer, S. Kralj, and M. Vilfan, J. Chem. Phys. **91**, 6411 (1989); N. Vrbancic *et al.,* J. Chem. Phys. **98**, 3540 (1993).
[7] G. P. Crawford, D. K. Yang, S. Žumer, D. Finotello, and J. W. Doane, Phys. Rev. Lett. **66**, 723 (1991); G. P. Crawford *et al., ibid.* **70**, 1838 (1993).
[8] G. Liu, Y. Li, and J. Jonas, J. Chem. Phys. **95**, 6892 (1991).
[9] K. R. Brownstein and C. E. Tarr, Phys. Rev. **19**, 2446 (1979).
[10] A. Abragam, *The Principles of Nuclear Magnetism* (The Clarendon Press, Oxford, 1961).
[11] B. Bak, J. Org. Chem. **21**, 797 (1956); J. P. Kintzinger, Mol. Phys. **30**, 673 (1975).
[12] M. Fury, S. G. Huang, and J. Jonas, J. Chem. Phys. **70**, 1260 (1979).
[13] W. T. Huntress, J. Chem. Phys. **48**, 3524 (1968).
[14] M. Brown, J. Chem. Phys. **77**, 1576 (1982).
[15] G. Lipari and A. Szabo, J. Am. Chem. Soc. **104**, 4546 (1982).